specific transporter and multi-drug resistance genes. Hum Mol Genet 7:597–608
Deltour L, Montagutelli X, Guenet JL, Jami J, Paldi A (1995) Tissue- and developmental stage-specific imprinting of the mouse proinsulin gene, Ins2. Dev Biol 168:686–688
Ekstroem TJ, Cui H, Li X, Ohlsson R (1995) Promoter specific IGF2 imprinting status and its plasticity during human liver development. Development 121:309–316
Ferguson-Smith AC, Cattanach BM, Barton SC, Beechey CV, Surani MA (1991) Embryological and molecular investigations of parental imprinting on mouse chromosome 7. Nature 351:667–670
Giddings SJ, King CD, Harman KW, Flood JF, Carnaghi LR (1994) Allele specific inactivation of insulin 1 and 2, in the mouse yolk sac, indicates imprinting. Nat Genet 6:310–313
Hayward BE, Moran V, Strain L, Bonthron DT (1998) Bidirectional imprinting of a single gene: GNAS1 encodes maternally, paternally, and biallelically derived proteins. Proc Natl Acad Sci USA 95:15475–15480
Kaneko-Ishino T, Kuroiwa Y, Miyoshi N, Kohda T, Suzuki R, Yokoyama M, Viville S, et al (1995) Peg1/Mest imprinted gene on chromosome 6 identified by cDNA subtraction hybridization. Nat Genet 11:52–59
Kobayashi S, Kohda T, Miyoshi N, Kuroiwa Y, Aisaka K, Tsutsumi O, Kaneko-Ishino T, et al (1997) Human PEG1/MEST, an imprinted gene on chromosome 7. Hum Mol Genet 6:781–786
Lefebvre L, Viville S, Barton SC, Ishino F, Keverne EB, Surani MA (1998) Abnormal maternal behaviour and growth retardation associated with loss of imprinted gene Mest. Nat Genet 20:163–169
Lefebvre L, Viville S, Barton SC, Ishino F, Surani MA (1997) Genomic structure and parent-of-origin-specific methylation of Peg1. Hum Mol Genet 6:1907–1915
Pan Y, McCaskill CD, Thompson KH, Hicks J, Casey B, Shaffer LG, Craigen WJ (1998) Paternal isodisomy of chromosome 7 associated with complete situs inversus and immotile cilia. Am J Hum Genet 62:1551–1555
Peters J, Wroe SF, Wells CA, Miller HJ, Bodle D, Beechey CV, Williamson CM, et al (1999) A cluster of oppositely imprinted transcripts at the Gnas locus in the distal imprinting region of mouse chromosome 2. Proc Natl Acad Sci USA 96:3830–3835
Reik W, Maher ER (1997) Imprinting in clusters: lessons from Beckwith-Wiedemann syndrome. Trends Genet 13:330–334
Riesewijk AM, Hu L, Schulz U, Tariverdian G, Hoglund P, Kere J, Ropers HH, et al (1997) Monoallelic expression of human PEG1/MEST is paralleled by parent-specific methylation in fetuses. Genomics 42:236–244
Sado T, Nakajima N, Tada M, Takagi N (1993) A novel mesoderm-specific cDNA isolated from a mouse embryonal carcinoma cell line. Dev Growth Differ 35:551–560
Spence JE, Perciaccante RG, Greig GM, Willard HF, Ledbetter DH, Hejtmancik JF, Pollack MS, et al (1988) Uniparental disomy as a mechanism for human genetic disease. Am J Hum Genet 42:217–226
Vu TH, Hoffman AR (1994) Promoter-specific imprinting of the human insulin-like growth factor-II gene. Nature 371: 714–717

Address for correspondence and reprints: Dr. Kenjiro Kosaki, Division of Medical Genetics, Department of Pediatrics, Keio University School of Medicine, 35 Shinanomachi, Shinjuku-ku, Tokyo 160-8582, Japan. E-mail: kkosaki@med.keio.ac.jp

0002-9297/2000/6601-0031$02.00

Am. J. Hum. Genet. 66:312–319, 2000

Involvement of the HLXB9 Homeobox Gene in Currarino Syndrome

To the Editor:

Anorectal malformations (ARMs) are among the most common congenital anomalies, accounting for 25% of digestive malformations that require neonatal surgery. ARMs have been found associated with sacral anomalies ~29% of the time (Rich et al. 1988). When ARMs are combined with lumbosacral anomalies, they fall into the spectrum of the caudal regression syndrome (CRS), which can also exhibit additional features such as partial or total sacrococcygeal agenesis, neural changes, and urogenital malformations (Lerone et al. 1997). The incidence of CRS is ~1 in 7,500 (Kallen et al. 1974). A detailed clinical characterization of patients affected by ARMs with partial or total sacrococcygeal agenesis revealed significant differences in the phenotypes, leading to the differentiation of five specific categories (Kalitzki 1965; Cama et al. 1996): (1) total sacral agenesis with normal or short transverse pelvic diameter and some lumbar vertebrae possibly missing (fig. 1*a* and *b*), (2) total sacral agenesis without involvement of lumbar vertebrae, (3) subtotal sacral agenesis or sacral hypodevelopment (with S1 present), (4) hemisacrum (fig. 1*c*), and (5) coccygeal agenesis.

In 1981, Guido Currarino described a form of CRS with hemisacrum (type IV sacral malformation), anorectal malformation, and presacral mass (anterior meningocele, teratoma, and/or rectal duplication) (fig. 1*d;* Currarino et al. 1981). The Currarino syndrome (CS; also called "Currarino triad") was observed to segregate in an autosomal dominant manner that often displayed phenotypic variability. As defined in the original reports, patients affected by true CS always exhibit the typical hemisacrum, with intact first sacral vertebra (sickle-shaped sacrum), which makes this specific sacral anomaly distinct to this syndrome.

Genetic studies suggested that a locus involved in normal sacral and anorectal development mapped to the terminal end (q36) of human chromosome 7 (Lynch et al. 1995; Seri et al. 1999). Mutations within the HLXB9 gene were identified in six cases, collectively grouped as

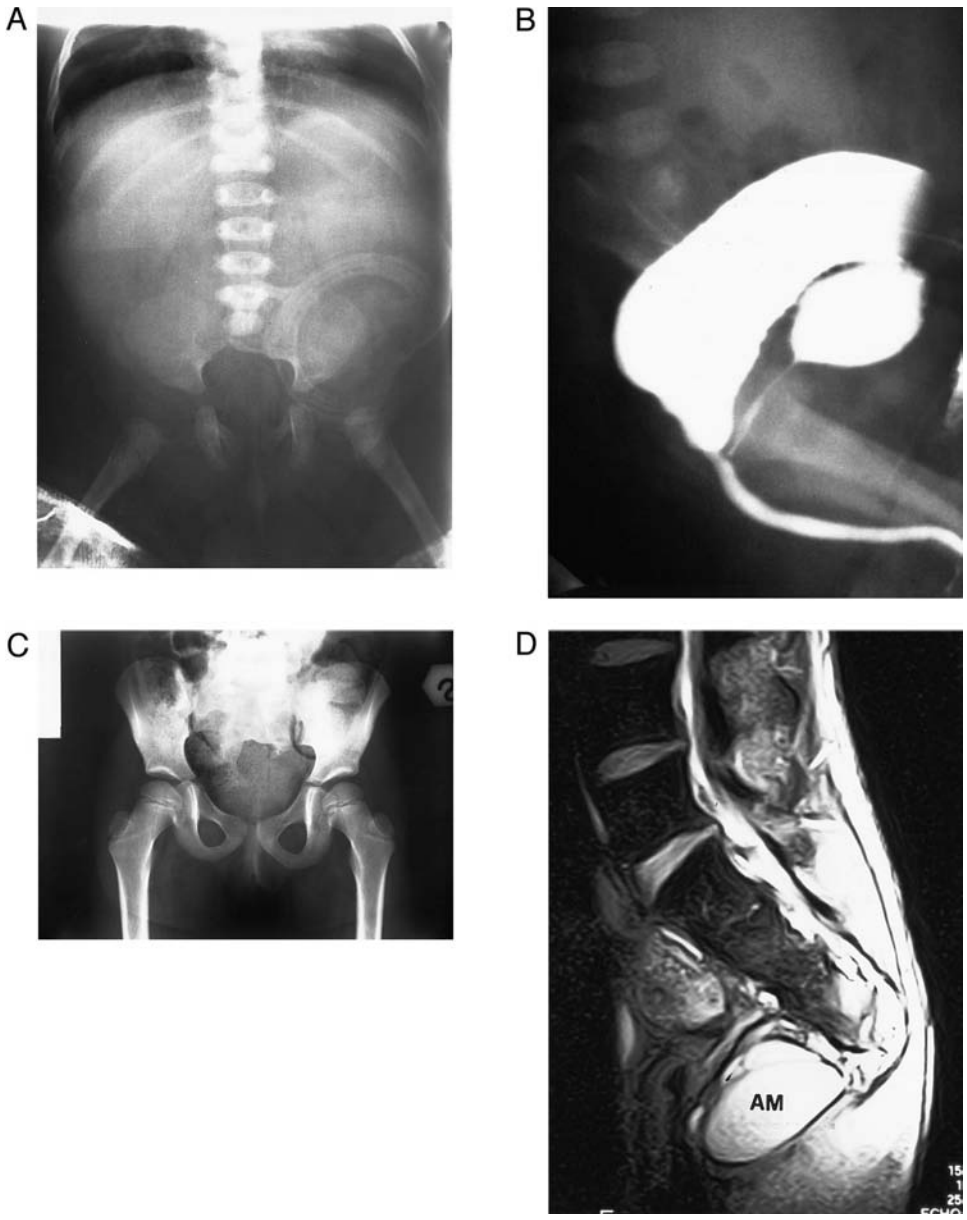

Figure 1 *a,* ARM with total sacral agenesis and L5 hypoplasia in patient 020. *b,* Distal cologram, showing presence of a rectobulbar fistula. *c* and *d,* Hemisacrum as observed in CS (*c*) and in patient 015 (*d*). The MRI shows the presence of the anterior meningocele (AM).

having dominantly inherited sacral agenesis (Ross et al. 1998). To define a more precise involvement of HLXB9 in the different phenotypic subgroupings of ARMs associated with sacral abnormalities, we screened for the presence of mutations in 27 individuals showing different sacral conditions, as described in table 1.

The HLXB9 gene contains three exons: double-gradient–denaturing gradient-gel electrophoresis (DG-DGGE) (Cremonesi et al. 1997) was performed on exons 2 and 3 (the homeodomain is coded by a portion of these two exons) (fig. 2). Patients showing an abnormal electrophoretic pattern were further analyzed by DNA sequencing (see conditions in the note to table 1). The DG-DGGE methodology yielded a high mutation-detection efficiency for exons 2 and 3, as reported elsewhere for the analysis of other genes (Cremonesi et al. 1999). Nevertheless, because of an extremely high melting profile for exon 1, it was necessary to sequence it in all 27 samples.

Analysis of the HLXB9 coding region and intron-exon

Table 1

Collection of Patients with Anorectal and Sacral Anomalies in This Study

Patient (Sex)	Clinical Diagnosis (Category)	Sacral Phenotype[a]	Associated Anomalies	HLXB9 Status/Predicted Protein Change	CGC Status
001 (F)	CS (IV)	Hemisacrum	ARM with rectoperineal fistula, presacral teratoma, tethered cord, anterior meningocele	Apparent hemizygous deletion of HLXB9	11/del
002 (F)	CS (IV)	Hemisacrum	ARM with rectoperineal fistula, anterior meningocele	384delG (exon 1)/truncated protein	11/11
011 (F)	CS (IV)	Hemisacrum	ARM with rectoperineal fistula, tethered cord, anterior meningocele, hydromyelia	R295W (exon 3/a), amino acid substitution within homeodomain	11/9
015 (M)	CS (IV)	Hemisacrum	ARM with rectoperineal fistula, anterior meningocele	Not detected	11/11
019 (M)	CS (IV)	Hemisacrum	ARM without fistula, hyposadia, Down syndrome	Not detected	11/9
059 (F)	CS (IV)	Hemisacrum	ARM with rectoperineal fistula, decreased bladder capacity	858+1G→A (exon 2)/splicing defect	11/11
060 (F)	CS (IV)	Hemisacrum	ARM with rectoperineal fistula	T248S (exon 2)/amino acid substitution within the homeodomain	11/11
066 (F)	CS (IV)	Hemisacrum	ARM with rectoperineal fistula, presacral teratoma	Not detected	11/11
069 (F)	CS (IV)	Hemisacrum	ARM, tethered cord, presacral mass, rectal duplication, bifid clitoris,lipoma of conus, holoprosencephaly	Hemizygous deletion of HLXB9	12/del
070 (M)	CS (IV)	Hemisacrum	ARM, presacral mass	Hemizygous deletion of HLXB9	11/del
003 (M)	CRS (III)	Agenesia of coccix and one sacral vertebra; SR = .43	ARM with rectobulbar fistula, lipoma of filum, hydromyelia, vertebral anomalies (L3–L4), syndactyly of second and third toes	Not detected	11/11
004 (M)	CRS (III)	Agenesia of coccix and one sacral vertebra; SR = .70	ARM with rectobulbar fistula, bilateral vesicoureteral reflux, vertebral anomalies (L2–L5)	Not detected	11/11
007 (M)	CRS (III)	SR = .55	ARM with rectoprostatic fistula, lipoma of terminal filum, hydromyelia, tethered cord, intra-atrial defect, pulmonary artery stenosis, syndactyly of the third and fourth fingers	Not detected	11/11
014 (M)	CRS (III)	CRS; SR = .45	ARM with rectovesical fistula	Not detected	11/11

(*continued*)

Table 1 Continued

Patient (Sex)	Clinical Diagnosis (Category)	Sacral Phenotype[a]	Associated Anomalies	HLXB9 Status/Predicted Protein Change	CGC Status
016 (F)	CRS (III)	Agenesia of coccix and one sacral vertebra; SR = .35	ARM with rectocloacal fistula, duplication of uterus and vagina	Not detected	11/11
018 (M)	CRS (III)	CRS	ARM with rectobulbar fistula, posterior meningocele	Not detected	11/11
024 (F)	CRS (III)	SR = .24	ARM with rectocloacal, lipoma of terminal filum, tethered cord, right ureterocele, intra-abdominal testis, bilateral congenital clubfoot	Not detected	11/10
025 (M)	CRS (III)	Agenesia of coccix and one sacral vertebra; SR = .54	ARM with rectobulbar fistula, intra-ventricular defect	Not detected	11/8
029 (F)	CRS (III)	Agenesia of coccix and three sacral vertebrae; SR = .33	ARM with rectoperineal fistula, high medullary cone (D11), vertebral fusion (L4–L5), annular pancreas, inferior limb arthrogryposis, bilateral congenital clubfoot	Not detected	11/11
030 (F)	CRS (III)	Agenesia of coccix and one sacral vertebra; SR = .58	ARM with rectocloacal fistula, tethered cord, L5 schisis, bicornate uterus	Not detected	11/11
031 (F)	CRS (III)	SR = .54	ARM with rectovestibular fistula, macrocrania	Not detected	11/11
033 (F)	CRS (III)	SR = .55	ARM with rectovestibular fistula, thickened filum terminale, tethered cord, hemangiomatosis	Not detected	11/9
035 (F)	CRS (III)	SR = .56	ARM with rectobulbar fistula, mild atrophy of cerebral cortex, hypoparathyroidism	Not detected	11/11
036 (M)	CRS (III)	Agenesia of coccix; SR = .54	ARM with rectobulbar fistula, low medullary cone (L4), open foramen ovale, right Hydronephrosis, anomalies of cervical spine and first right rib	Not detected	11/11
068 (F)	CRS (III)	SR = .27	ARM with rectocloacal fistula, monolateral renal dysgenesis	Not detected	11/11
009 (M)	Sacral agenesis (I)	Complete sacral agenesis	ARM with rectoprostatic fistula, high medullary cone (D11), hydromyelia, right multicystic kidney, left mega-ureter, right hernia and undescended testis	Not detected	11/11

(*continued*)

Table 1 Continued

Patient (Sex)	Clinical Diagnosis (Category)	Sacral Phenotype[a]	Associated Anomalies	HLXB9 Status/Predicted Protein Change	CGC Status
020 (M)	Sacral agenesis (I)	Agenesis of sacral vertebrae and one lumbar vertebra	ARM with rectobulbar fistula, bilateral congenital clubfoot, monolateral renal dysgenesis, hypospadias	Not detected	11/11

NOTE.—In the familial cases (001, 015, 059, and 060) where mutations are detected, they segregate with the phenotype. The exception is the mother of patient 060, who has the T248S change but no detectable phenotype. The following polymorphic markers were used to define the extent of the deletion in patients 069 and 070: cen-NOS3-D7S1829-GATAP6678-D7S1491-D7S798-D7S2546-AFM175yg1-D7S637-D7S2462-D7S550-SHH-D7S2465-D7S559-HLXB9-D7S2423-D7S594-tel (see Chromosome 7 Database; for a high-resolution map around SHH and HLXB9, see the work of Belloni et al. [1996] and Heus et al. [1999]). The breakpoints in patients 069 and 070 were located between markers D7S550–D7S2465 (centromeric) and D7S2423–D7S594 (telomeric) and between markers NOS3–D7S1829 (centromeric) and D7S2423–D7S594 (telomeric), respectively, indicating that HLXB9 was deleted in both patients. DG-DGGE conditions were as follows: exon 2—60%–100% urea-formamide (in all cases, 7M urea and 40% formamide represent the 100% denaturant), 6.5%–12% acrylamide, 75 V, 16 h, for primers HB9-2F (5′-TGTAGTGGTACAATCAGCAACGGGA-3′) and HB9-2R (5′-GCCCGCCCCCGCCGCCCTGCCCGCGCCCCGCGCCGCCCGCTCGCCGCCCGCCGCCCGCAAAGGTAACAGTGTCCCATGGGA-3′) (351-bp product); the PCR was 94°C for 5 min (1 cycle); 94°C for 1 min, 60°C for 45 s, and 72°C for 1 min (35 cycles); and 72°C for 10 min (1 cycle); exon 3/a—40%–90% urea, 6.5%–15% acrylamide, 50 V, 14 h, for primers HB9-3/aF (5′-GCCCGCCCCCGCCGCCCTGCCCGCGCCCCGCGCCGCCCGCTCGCCGCCCGCCGCCCCCTTCTGTTTCTCCGCTTCCTGCG-3′) and HB9-3aR (5′ CACCCTGAGGCCATTCCAGGGCCGA-3′) (266-bp product); the PCR was 94°C for 5 min (1 cycle); 94°C for 1 min, 60°C for 45 s, and 72°C for 1 min (35 cycles); and 72°C for 10 min (1 cycle); exon 3/b—30%–100% urea, 10%–15% acrylamide, 65 V, 20 h, for primers HB9-3/bF (5′CCCGCCGCCCGCCGCTCGCCCGCCGCGCCCCGCGCCCGTCCCGCCGCCCCCGCCCAAAAAAGGCCAAAGAGCAGG-3′) and HB9-3/bR (5′-TGCGGGCGCCGGGGCCTCCGGGAGA-3′) (446-bp product). The PCR was 94°C for 5 min (1 cycle); 94°C for 1 min, 62°C for 45 s, and 72°C for 1 min (35 cycles); and 72°C for 10 min (1 cycle). Primer pairs used for amplification and sequencing of exon 1 (with an ABI-373) were HB9-1F (5′-CCGCACACGGCCGCGTCGCCCGCCACCGGG-3′) and HB9-1R (5′-CGGCGGCGGCAGCGGCCGCTGCGCCCGGAT-3′) (439-bp product) (the PCR was 94°C for 5 min [1 cycle]; 94°C for 1 min, 60°C for 45 s, and 72°C for 1 min [35 cycles]; and 72°C for 10 min [1 cycle]) and HB9-1FaM13 (5′-TGTAAAACGACGGCCA-GTCGGCACGGGCGGCGGGCACGGGGGGCCCCA-3′) and HB9-1Rc (5′-GCAGCTCTTCCCCCGCTCGCTGGGAGCCAA-3′) (518-bp product); the PCR was 94°C for 5 min (1 cycle); 94°C for 1 min, 62°C for 45 s, and 72°C for 1 min (35 cycles); and 72°C for 10 min (1 cycle). PCR-mediated site-directed mutagenesis experiments were designed to detect the 384delG mutations by use of the following primers: HB9-1F-PSDM (5′-GCCCGCCGACCGCCTGCGCGCCGAGAGGCC-3′) and HB9-1R (179-bp product); the PCR was 94°C for 5 min (1 cycle); 94°C for 1 min, 58°C for 45 s, and 72°C for 1 min (30 cycles); and 72°C for 10 min (1 cycle). *Stu*I restriction digestion of the precipitated PCR products recognizes the presence of the restriction site only on the mutated allele (50 μl of PCR product were precipitated and digested with *Stu*I; undigested fragment, 179 bp; digested fragments, 28 and 151 bp). Analysis was on a 2% agarose/1% Nu-Sieve gel. Each PCR reaction was performed on 500 ng of genomic DNA in a 50-μl volume containing 50 pmol of each primer, 400 mmol of each dNTP, 10% dimethyl sulfoxide, 1 U of Dynazyme DNA polymerase, 10 mM TRIS-HCl (pH 8.8), 1.5 mM $MgCl_2$, 50 mM KCl, and 1.5% Triton X-100. Analysis of the CGC repeat coding for the polyalanine tract was accomplished by PCR of the region (Eppendorf *Pfu*), followed by electrophoresis on 6% polyacrylamide. Primers HB9-1Fa and HB9-1Rrep (5′-AGGGTGCAGCCCCAGCGCCAGGCC-3′) were used. One of the two primers was end-labeled with $\gamma[^{32}P]$-dATP, by means of NEB T4 kinase (in a 10-μl reaction: primer, 100 pmol; T4 kinase, 5 U; T4 buffer, 1 μl; and $\gamma[^{32}P]$-dATP, 10 mCi; the labeling was for 1 h at 37°C, followed by precipitation such that the primer was at the final concentration of 4 pmol/ml); the PCR was 94°C for 5 min (1 cycle); 94°C for 1 min, 60°C for 45 s; and 72°C for 1 min (30 cycles); 60°C for 45 s; and 72°C for 10 min (1 cycle) and was performed on 250 ng of genomic DNA in a 25-μl reaction mixture containing 4 pmol of labeled primer, 20 pmol of unlabeled primer, 400 mmol of each dNTP, 10% dimethyl sulfoxide, and 1.25 U of *Pfu,* 20 mM TRIS-HCl (pH 8), 2 mM $MgCl_2$, 10 mM KCl, 6 mM $(NH_4)_2SO_4$, 0.1% Triton X-100, and 10 mg nuclease-free BSA/ml. Four microliters of each reaction was run on polyacrylamide gels for 4 h at 1,800 V. M13mp18 sequence was used as a length control for the PCR product that was 124 bp in the presence of the CGC_{11} repeated unit.

[a] SR = sacral ratio. This is obtained by comparison of the sacrum size with the fixed bony parameter of the pelvis, creating a ratio between different segments (Pena 1995); the normal SR is .77.

boundaries in our cohort of patients detected mutations in only those clinically characterized to have CS. Four patients (002, 011, 059, and 060) harbored, within the coding sequence, heterozygous point mutations that would be predicted to cause deleterious changes in the protein (table 1). The entire HLXB9 gene in two patients (069 and 070) and possibly a third (001; see below) was found to be deleted. For each mutation, a similar change was not observed in any of 100 normal chromosomes examined either through DG-DGGE (T248S, 858 +1G→A, R295W) or PCR-mediated site-directed mutagenesis (384delG) (Haliassos et al. 1989). DG-DGGE of exon 2 detected the presence of an abnormal pattern in 1 of 100 normal and 1 of 54 patient chromosomes examined: direct sequencing showed that the sequence variation is intronic and not involved in the splicing. Moreover, the DNA sequence of exon 1 in patient 059, already affected by the 858+1G→A mutation, contained, at position 357, a second nucleotide change, which does not cause an amino acid change (P119P).

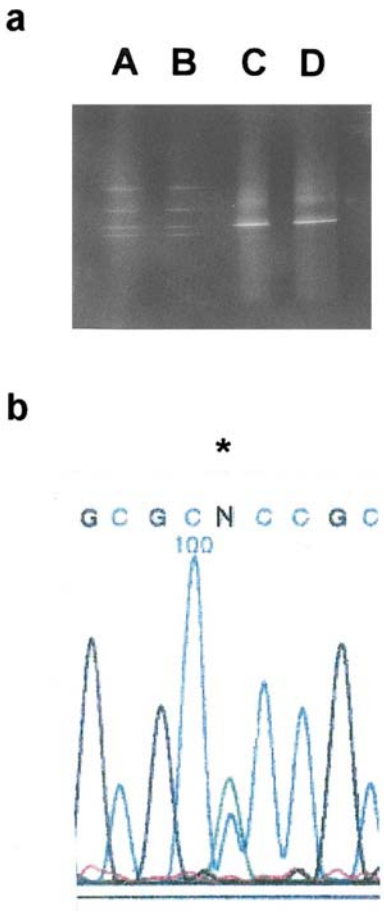

Figure 2 Example of DG-DGGE (*a*) and direct DNA sequencing (*b*). *a,* Lanes A and B, Replicated samples frm patient 060. Lanes C and D, Controls. *b,* Electrophoregram showing two peaks (marked with an asterisk [*]) at the T248S mutation in patient 060.

The missense mutations all affect the homeodomain, suggesting that an amino acid change in this region is relevant to the normal functioning of the protein. The 858+1G→A mutation affects a nucleotide in the donor splicing site, which is 100% conserved, suggesting that an abnormal protein will be obtained in this case.

We also analyzed the region of exon 1, coding for the 16-alanine stretch, since variation in polyalanine residues has been reported in other homeobox genes involved in disease (Goodman et al. 1997; Mundlos et al. 1997; Brais et al. 1998). This region, which includes a CGC repeat, was examined to test if length variation was associated with any phenotype in our collection (87 unaffected individuals, or 174 chromosomes, served as controls). We determined that the CGC_{11} allele was the most common in the general population, accounting for the 90.23% of the chromosomes analyzed. Other alleles observed were CGC_{12} (1.7%), CGC_9 (7.47%), and CGC_8 (0.6%), and these were all heterozygous changes. Only one sample (including both affected individuals and controls) revealed a homozygous change in the polyalanine tract (CGC_9/CGC_9). Although this sample was from the control collection, closer investigation revealed that the individual lacked fusion of the posterior arch of the vertebrae and had scoliosis on the left side. No association between the CGC-repeat length and the presence of sacral malformations could be established, since the alleles observed in the 27 patients were all detected in controls.

The CGC-repeat length was important in the analysis of CS sample 001, the one family, of our collection, demonstrating linkage to 7q36 (Seri et al. 1999). In this family, the CGC_9 allele has not been passed from the 2d to the 3d generation, which suggests that a microdeletion involving HLXB9 or an expansion of the allele from CGC_9 to CGC_{11} was present in two affected brothers of the 2d generation and then was transmitted to their descendants. Since an expansion would not likely be pathogenic (on the basis of our other findings), it is more likely that a microscopic deletion occurred. FISH analysis, with BACs and cosmids encompassing HLXB9, give the expected two signals on metaphase analysis (data not shown), which would suggest that the microdeletion is small. In three patients with CS (015, 019, and 066), no DNA sequence alterations were detected.

Therefore, we identified HLXB9 mutations in only those individuals diagnosed as having CS. This observation is not inconsistent with the findings of the original report (Ross et al. 1998), which described six different mutations in unrelated individuals who either were diagnosed with CS or had partial characteristics reminiscent of CS. (These patients, however, were all collectively grouped as having sacral agenesis.) Instead, it refines the involvement of HLXB9 in specific anorectal and sacral malformations. Thus, we have not been able to demonstrate a role for HLXB9 in caudal regression (categories III and V) and total sacral agenesis (categories I and II). Although it is possible that a mutation or DNA sequence variation in the noncoding region of HLXB9 could be present in these individuals, it is perhaps more likely that these malformations are due to other factors or defects in other gene(s). In three patients with CS (015, 019, and 060), no mutation could be found, which suggests genetic heterogeneity in CS or some other nongenetic determinant (since these cases are all sporadic and not familial). To our knowledge, no linkage studies of families affected exclusively by CRS or total sacral agenesis have been reported so far. The use of mouse models to study the human disease will likely be limited, since mice homozygous for a null mutation in Hlxb9 apparently fail to show any sacral defect (Harrison et al. 1999; Li et al. 1999)

In the mutation screen, we paid particular attention to the polyalanine region in exon 1, since variation in

lengths of these tracts in other homeodomain genes have been described in specific pathologies such as synpolydactyly (Mundlos et al. 1997), oculopharyngeal muscular dystrophy (Brais et al. 1998), and cleidocranial dysplasia (Goodman et al. 1997). Although we could determine that the CGC_{11} allele was the most common in the population (~90%), there was no specific correlation with any heterozygous variants (which led to either an increase or a decrease in CGC length) in the sacral conditions studied. A homozygous reduction in the length of the repeat (CGC_9/CGC_9) was identified in a single control sample, and, although this individual exhibited spinal anomalies, a clear correlation could not be established and will require further investigation.

In most ARMs and sacral-defect cases, the cause is unknown, and no familial recurrence is noted. In spite of the small number of familial cases reported, it is possible that specific genes cause defined phenotypes. In this study, we have presented evidence that the HLXB9 may be exclusively involved in CS. This observation is immediately relevant for clinical investigation and genetic screening, and the criteria and protocols to perform these studies have been outlined in this report.

Acknowledgments

This work has been supported by "Fondazione Telethon Italia" grant 297/bi, the Italian Ministry of Health, "Ricerca Finalizzata, 1996," and the Medical Research Council of Canada (MRC). We are grateful to patients and families who provided samples for our analysis. The authors would also like to acknowledge Peter Heutink, Carol Stayton, Massimiliano Agnelli, Silvia Presi, Elena Rossi, Roberta Cinti, and the PRIMM Sequencing Facility, for technical support, and Drs. Jean Michel Guys, Armando Cama, Margherita Lerone, Romeo Carrozzo, Victoria Maria Siu, and Hironao Numabe, for clinical evaluation. L.-C. T. is a Senior Scientist, and S.W.S. is a Scholar, of the MRC.

E. Belloni,[1,*] G. Martucciello,[2] D. Verderio,[1] E. Ponti,[1] M. Seri,[2] V. Jasonni,[2] M. Torre,[2] M. Ferrari,[1] L.-C. Tsui,[3] and S. W. Scherer[3]

[1]*Istituto di Ricovero e Cura a Carattere Scientifica, Hospital San Raffaele, Genetics and Molecular Diagnostic Unit, Milan;* [2]*"Giannina Gaslini" Institute, University of Genoa, Genoa; and* [3]*Department of Genetics, The Hospital for Sick Children, Toronto*

Electronic-Database Information

The URL for data in this article is as follows:

Chromosome 7 Database, The, http://www.genet.sickkids.on.ca/chromosome7

References

Belloni E, Muenke M, Roessler E, Traverso G, Siegel-Bartelt J, Frumkin A, Mitchell HF, et al (1996) Identification of *Sonic hedgehog* as a candidate gene responsible for holoprosencephaly. Nat Genet 14:353–356

Brais B, Bouchard JP, Xie YG, Rochefort DL, Chretien N, Tome FM, Lafreniere RG, et al (1998) Short GCG expansions in the PABP2 gene cause oculopharyngeal muscular dystrophy. Nat Genet 18:164–167

Cama A, Palmieri A, Capra V, Piatelli GL, Ravegnani M, Fondelli P (1996) Multidisciplinary management of caudal regression syndrome. Eur J Pediatr Surg 6:44–45

Cremonesi L, Firpo S, Ferrari M, Righetti PG, Gelfi C (1997) Double-gradient DGGE for optimized detection of DNA point mutations. Biotechniques 22:326–330

Cremonesi L, Carrera P, Fumagalli A, Lucchiari S, Cardillo E, Ferrari M, Righetti SC, et al (1999) Validation of double gradient denaturing gradient gel electrophoresis through multigenic retrospective analysis. Clin Chem 45:35–40

Currarino G, Coln D, Votteler T (1981) Triad of anorectal, sacral, and presacral anomalies. Am J Roentgenol 137: 395–398

Goodman FR, Mundlos S, Muragaki Y, Donnai D, Giovannucci-Uzielli ML, Lapi E, Majewski F, et al (1997) Synpolydactyly phenotypes correlate with size of expansions in HOXD13 poly-alanine tract. Proc Natl Acad Sci USA 94: 7458–7463

Haliassos A, Chomel JC, Tesson L, Baudis M, Kruh J, Kaplan JC, Kitzis A (1989) Modification of enzymatically amplified DNA for the detection of point mutations. Nucleic Acids Res 17:3606

Harrison KA, Thaler J, Pfaff SL, Gu H, Kehrl JH (1999) Pancreas dorsal lobe agenesis and abnormal islets of Langerhans in Hlxb9-deficient mice. Nat Genet 23:71–75

Heus HC, Hing A, van Baren MJ, Joosse M, Breedveld GJ, Wang JC, Scherer SW, et al (1999) A physical and transcriptional map of the preaxial polydactyly locus on chromosome 7q36. Genomics 57:342–351

Kalitzki M (1965) Congenital malformations and diabetes. Lancet 2:641–642

Kallen B, Windberg I (1974) Caudal mesoderm pattern of anomalies: from renal agenesis to sirenomelia. Teratology 9:99–112

Lerone M, Bolino A, Martucciello G (1997) The genetics of anorectal malformations: a complex matter. Semin Pediatr Surg 6:170–179

Li H, Arber S, Jessell TM, Edlund H (1999) Selective agenesis of the dorsal pancreas in mice lacking homeobox gene Hlxb9. Nat Genet 23:67–70

Lynch SA, Bond PM, Copp AJ, Kirwan WO, Nour S, Balling R, Mariman E, et al (1995) A gene for autosomal dominant sacral agenesis maps to the holoprosencephaly region at 7q36. Nat Genet 11:93–95

Mundlos S, Otto F, Mundlos C, Mulliken JB, Aylsworth AS, Albright S, Lindhout D, et al (1997) Mutations involving the transcription factor CBFA1 cause cleidocranial dysplasia. Cell 89:773–779

Pena A (1995) Anorectal malformations. Semin Pediatr Surg 4:35–47

Rich AM, Brock WA, Pena A (1988) Spectrum of genitourinary malformations in patients with imperforate anus. Pediatr Surg Int 3:110–113

Ross AJ, Ruiz-Perez V, Wang Y, Hagan D-M, Scherer S, Lynch SA, Lindsay S, et al (1998) A homeobox gene, HLXB9, is the major locus for dominantly inherited sacral agenesis. Nat Genet 20:358–361

Seri M, Martucciello G, Paleari L, Bolino A, Priolo M, Salemi G, Caroli F, et al (1999) Exclusion of the *Sonic Hedgehog* gene as responsible for Currarino syndrome and anorectal malformations with sacral hypodevelopment. Hum Genet 104:108–110

* Present affiliation: Department of Experimental Oncology, Institute of Oncology, Milan.

Address for correspondence and reprints: Dr. Steve Scherer, Department of Genetics, Room 9107, The Hospital for Sick Children, 555 University Avenue, Toronto, Ontario M5G 1X8, Canada. E-mail: steve@genet.sickkids.on.ca

0002-9297/2000/6601-0032$02.00

Am. J. Hum. Genet. 66:319–326, 2000

A Novel Locus for Leber Congenital Amaurosis Maps to Chromosome 6q

To the Editor:

Leber congenital amaurosis (LCA) (MIM 204000/204100) is a clinically and genetically heterogeneous retinal disorder that occurs in infancy and is accompanied by profound visual loss, nystagmus, poor pupillary reflexes, and either a normal retina or varying degrees of atrophy and pigmentary changes (Leber 1869, 1871; François 1968). The electroretinogram (ERG) is extinguished or severely reduced (Franceschetti 1954). LCA is largely a recessive disease, although autosomal dominant pedigrees have been identified (Sorsby et al. 1960; Heckenlively 1988). To date, three genes for LCA have been identified and sequenced: retinal guanylate cyclase (*GUCY2D*) on chromosome 17p13; retinal pigment epithelium protein (*RPE65*) on chromosome 1p31; and cone-rod homeobox (*CRX*) on chromosome 19q13.3. One additional locus has been identified on chromosome 14q24 (Stockton et al. 1998). We show evidence for linkage to chromosome 6q11-16 in a multigenerational kindred of Old Order River Brethren. The disease gene maps to a 23-cM interval flanked by DNA polymorphic markers D6S1551 and D6S1694, with a maximum two-point LOD score of 3.38 (recombination fraction [θ] zero) at D6S391. Two candidate genes on chromosome 6 were screened for mutations: gamma aminobutyric acid rho1 and rho2 (*GABRR1* and *GABRR2*) at 6q14-21 (Cutting et al. 1992), and interphotoreceptor matrix proteoglycan (*IMPG1*) at 6q13-15 (Gehrig et al. 1998).

The incidence of LCA is 3 in 100,000 persons and accounts for $\geqslant$5% of all inherited retinal dystrophies (Perrault et al. 1996). Clinical and genetic heterogeneity have been demonstrated (Wardenburg 1961; Camuzat et al. 1996). The phenotype has been associated with familial juvenile nephronophthisis and cone-shaped epiphyses (Saldino-Mainzer syndrome) and with kidney disease (Senior-Loken syndrome), osteoporosis, metabolic diseases, and neurological abnormalities (Loken et al. 1961; Senior et al. 1961; Dekaban 1969; Mainzer et al. 1970; Ellis et al. 1984).

The first locus for LCA was mapped to 17p13 with the use of homozygosity mapping in consanguineous families of North African descent (Camuzat et al. 1996). Mutations in the retina-specific guanylate cyclase gene (*RETGC 1*), on chromosome 17p13, involved in phototransduction, were subsequently identified (Perrault et al. 1996). Mutations in *RPE65* on chromosome 1p31, specific to the retinal pigment epithelium involved in retinoid metabolism, were reported in patients with LCA, thus establishing a second gene (*LCA2*) for this heterogeneous disease (Marlhens et al. 1997). The photoreceptor-specific homeobox gene *CRX,* on chromosome 19q13.3, has been implicated as the third gene, since mutations were demonstrated (Freund et al. 1998). A novel locus on chromosome 14q24 (*LCA3*) was identified in consanguineous Saudi Arabian families (Stockton et al. 1998).

We studied a consanguineous family belonging to the Old Order River Brethren, a religious isolate originating in eastern Pennsylvania. The Old Order River Brethren descended from the Swiss, who emigrated to America in the 1750s in pursuit of religious freedom (Breckvill 1972). The kindred includes three affected individuals in two related sibships (fig. 1) who were initially evaluated at the Johns Hopkins Center for Hereditary Eye Diseases (JHCHED) and who are being followed annually. The patients presented with visual acuities in the order of 20/100–20/400, nystagmus, high hypermetropia, poor pupillary reflexes, and normal fundi. Progressive hypermetropia and increasing peripheral retinal mottling, of varying degree, were noted. The ERG was abolished. Review of other systems was unremarkable. We report a novel locus for LCA (*LCA5*) in this pedigree, on chromosome 6q11-16, by linkage analysis and homozygosity mapping.

Venous blood samples were obtained from 27 family members of the Old Order River Brethren community and a cheek brush sample was obtained from an infant (individual 29). Consents were obtained in accordance with regulations of the Johns Hopkins Medical Institutions' Joint Committee on Clinical Investigation. DNA was isolated from whole blood by means of the QIAamp Blood Kit (Qiagen), according to the manufacturer's in-